Transactions of Tianjin University (2023) 29:216–224
https://doi.org/10.1007/s12209-023-00356-z

RESEARCH ARTICLE

Fluorescence Turn-On/Off Responses of In (III)-MOF to Short-Chain Perfluorocarboxylic Acids

Jie Lv[1] · Yabo Xie[1] · Lin-Hua Xie[1] · Jian-Rong Li[1]

Received: 21 March 2023 / Revised: 14 April 2023 / Accepted: 20 April 2023 / Published online: 16 June 2023

Abstract

Short-chain perfluorocarboxylic acids (PFCAs) are a class of persistent organic pollutants that are widely used as substitutes for long-chain PFCAs. However, they also pose a non-negligible risk to ecosystems. In this study, we demonstrated that a fluorescent metal–organic framework (MOF) (named V-101) constructed from In^{3+} and an aromatic-rich tetratopic carboxylate ligand 5-[2,6-bis (4-carboxyphenyl) pyridin-4-yl] isophthalic acid (H_4BCPIA) exhibited highly efficient turn-off and turn-on fluorescence responses toward five short-chain PFCAs in water and methanol, respectively. The limits of detection of V-101 toward five short-chain PFCAs are down to μg/L level, and it showed good anti-interference abilities toward short-chain PFCAs in the presence of common metal ions. The major mechanisms associated with fluorescence responses were molecular collisions and interactions between V-101 and short-chain PFCAs. This work demonstrates that the structure variety of MOFs imparts them with the potential of MOFs in the detection of short-chain PFCAs for pollution control.

Keywords Perfluorocarboxylic acids · Fluorescent detection · Metal–organic framework (MOF)

Introduction

Perfluorocarboxylic acids (PFCAs) are widely used in the commercial and industrial production of many products (such as coating formulations, fire-fighting foams, inks, varnishes, lubricants, water proofer, paper, and textiles) due to their excellent surface activity, high thermal, chemical stability, and high light transmittance [1]. PFCAs are difficult to be decomposed in the natural environment, they exhibit strong persistence and are easily ingested and accumulated in living organisms [2]. The use of long-chain PFCAs ($C_nF_{2n+1}COOH$, $n \geq 7$) is regulated in many countries due to public concern about their toxicity following environmental enrichment [3, 4]. Short-chain PFCAs ($C_nF_{2n+1}COOH$, $n < 7$) are thus widely used as alternatives to long-chain PFCAs [5]. However, they have similar environmental persistence with long-chain PFCAs and are more mobile in the environment due to their higher solubility in water and lower sorption to solids [6–9].

It is well known that PFCAs show a very weak response in ultraviolet (UV) and fluorescence spectrophotometry, and are not easily detected by gas chromatography–mass spectrometry (GC–MS) because of the complexity of derivatization of these molecules in pretreatment [10]. Liquid chromatography–mass spectrometry (LC–MS) is most commonly used to detect PFCAs. However, it involves a complex sample pretreatment process, the instruments are expensive, and experienced personnel are required to operate the equipment. Therefore, it is necessary to develop a simple and rapid molecular recognition technique for detecting PFCAs.

Metal–organic frameworks (MOFs) have been proven to be an ideal platform for the detection and removal of PFCAs due to their high porosity, surface tunability, high selectivity, and sensitivity [11–14]. In this respect, Wriedt and coworkers investigated the adsorption properties of NU-1000 for three perfluorosulfonic acids (PFSAs) and six PFCAs from aqueous solutions [15]. The results indicated that NU-1000 exhibited outstanding adsorption capacities for PFSAs (400–620 mg/g) and PFCAs (201–604 mg/g), and it showed

PFCAs are toxically chemicals and should be handled carefully, and the measurements should be carried out in the professional laboratory!

✉ Lin-Hua Xie
xielinhua@bjut.edu.cn

✉ Jian-Rong Li
jrli@bjut.edu.cn

[1] Beijing Key Laboratory for Green Catalysis and Separation, Department of Chemical Engineering, Beijing University of Technology, Beijing 100124, China

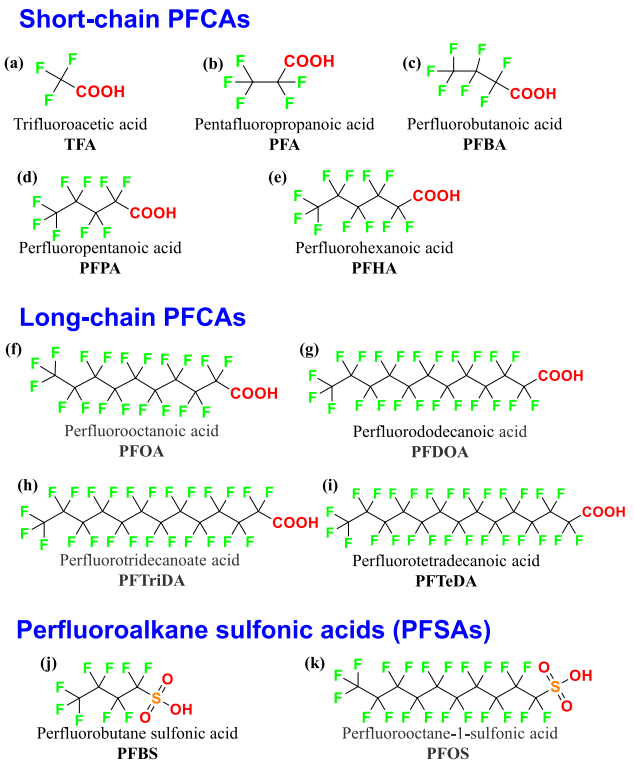

Fig. 1 Molecular structures of 11 typical perfluoroalkyl acids. **a–e** Short-chain PFCAs; **f–i** long-chain PFCAs; and **j**, **k** perfluoroalkane sulfonic acids (PFSAs)

ultrafast adsorption kinetics (equilibrium time of < 1 min). Li and coworkers prepared a water-stable luminescent MOF (LMOF) (named In (tcpp)) that showed a selective and strong luminescence-based turn-off detection ability for a long-chain PFCA (perfluorooctanoic acid (PFOA)) in water, with a limit of detection (LOD) of 19 μg/L [16]. The previous studies have shown that MOFs are promising candidates for removing perfluoroalkyl acids (PFAAs) and detecting a specific PFCA (PFOA). Short-chain PFCAs are now widely used to replace long-chain PFCAs, but few work has been reported to detect them in the environment using MOF as a convenient method.

In this study, we analyzed the ability of an LMOF $\{(Me_2NH_2)$ [In (BCPIA)]. 2DMF$\}_n$ (V-101) in the detection of PFCAs. The LMOF was synthesized using an organic ligand 5-[2, 6-bis (4-carboxyphenyl) pyridin-4-yl]isophthalic acid (H_4BCPIA) and In $(NO_3)_3$ in N,N-dimethylformamide (DMF) via a solvothermal reaction in accordance with a previously reported method [17]. V-101 exhibited strong fluorescence and high stability, and it was used to detect 11 PFAAs (Fig. 1), including five short-chain PFCAs: trifluoroacetic acid (TFA), pentafluoropropionic acid (PFA), perfluorobutanoic acid (PFBA), perfluoropentanoic acid (PFPA), and perfluorohexanoic acid (PFHA); four long-chain PFCAs: perfluorooctanoic acid (PFOA), perfluorododecanoic acid (PFDOA), perfluorotridecanoic acid (PFTriDA), and perfluorotetradecanoic acid (PFTeDA); and two perfluoroalkane sulfonic acids (PFSAs): perfluorobutane sulfonic acid (PFBS) and perfluorooctane-1-sulfonic acid (PFOS). V-101 showed highly sensitive fluorescence responses to the short-chain PFCAs. Interestingly, the fluorescence responses of V-101 toward short-chain PFCAs differed significantly in water (turn-off fluorescence) compared to methanol (turn-on fluorescence). The LODs of V-101 to TFA, PFA, PFBA, PFPA, and PFHA were estimated to be in the range of 8–23 μg/L in water and 10–146 μg/L in methanol.

Experimental

Materials and Instruments

All general chemicals and solvents (AR grade) were commercially available and used as received. The ligand H_4BCPIA was synthesized using a previously reported method [18]. Fourier transform infrared (FT-IR) data were measured using an FT-IR spectrophotometer (Shimadzu IR Affinity-1). Powder X-ray diffraction (PXRD) patterns were obtained at room temperature on a Rigaku SmartLab 3 X-ray powder diffractometer equipped with a Cu sealed tube ($\lambda = 1.54178$ Å). Photoluminescence spectra were recorded using an F-7000 FL fluorescence spectrophotometer at room temperature, and luminescence lifetimes were recorded by an FLS-100 steady-state/lifetime spectrofluorometer.

Synthesis of V-101

In $(NO_3)_3{\cdot}6H_2O$ (50 mg, 0.06 mmol), H_4BCPIA (35 mg, 0.05 mmol) and DMF (10 mL) were mixed in a 20-mL autoclave and ultrasonically dissolved. And then, 1-mL concentrated HNO_3 was added to the mixture, and the sealed autoclave was placed in a 120 °C oven for 48 h. After cooling the autoclave, yellow crystals were collected by centrifugation.

Activation of MOF Sample

The as-synthesized V-101 was immersed in fresh DMF at 80 °C for 2 d and then immersed in fresh acetone for another 2 d. During the soaking process, the two solvents were replaced by fresh ones 6 times. The MOF sample was then dried at room temperature under vacuum and degassed at 80 °C for 10 h using the Micromeritics VacPrep 061 sample degas system.

Fluorescence Measurements

Activated V-101 (5 mg) was ground and dispersed in 40-mL water or methanol to form a uniform suspension under sonication. Fluorescence titration experiments were carried out in a cuvette by incrementally adding aliquots of PFCAs solutions to 1-mL suspension of V-101, and its fluorescence spectra were recorded using a fluorescence spectrophotometer.

For the interference experiments, NH_4Cl, NaCl, $CaCl_2$, $Mg(NO_3)_2$, and KCl were added to the suspension of V-101, and the fluorescence of the mixture was recorded. Then, the fluorescence of the mixture was recorded after every incremental addition of the solution of TFA (100 mg/L).

For the sensing experiment using a real sample, 40-mL water from Moon Lake of Beijing University of Technology was used to prepare a suspension of V-101 and 100-mg/L TFA aqueous solution after centrifugation and filtration, respectively. The fluorescence titration experiments were carried out according to the above procedures, and the experiments were performed for 3 times. Two 20-mL vials were put into 200-mg toilet paper (JieRan brand), respectively, and one of the vials was spiked with 2.6 μL of TFA. Each of samples was extracted 4 times with 20-mL methanol by vortexing and sonication, and then, the methanol solution without TFA was used to make the suspension of V-101. The fluorescence titration experiment was performed 3 times.

Results and Discussion

Characterization of the MOF

V-101 was synthesized from $In(NO_3)_3$ and the ligand H_4BCPIA by solvothermal reaction. As shown in Fig. 2a and b, each In^{3+} in V-101 coordinated with four carboxylate groups from four different $BCPIA^{4-}$ ligands, forming an $In(CO_2)_4$ secondary building unit (SBU), and each $BCPIA^{4-}$ ligand is bridging four different $In(CO_2)_4$ SBUs. The alternative connection between In $(CO_2)_4$ SBUs and $BCPIA^{4-}$ ligands resulted in a three-dimensional (3D) network, and the twofold interpenetration of these 3D networks resulted in the framework structure of V-101 (Fig. 2c and d). There are two types of 1D channels, with diameters of approximately 6 Å and 4.5 Å along the *a* and *b* axes, respectively (Fig. S1a and b). The PXRD pattern of the as-synthesized V-101 was consistent with its simulated PXRD pattern (Fig. S2), which was indicative of successful preparation of V-101. Furthermore, after being immersed in water or methanol (MeOH) for 24 h, the PXRD patterns of the solvent-treated V-101 samples still matched those of the as-synthesized one (Fig. S2), which indicated that the crystalline structure of V-101 remained unchanged and that it was highly stable in relation to the solvents.

Detection of PFAAs

As PFAAs can be dissolved in water, and methanol is the most commonly used eluent and extractant of PFAAs in the

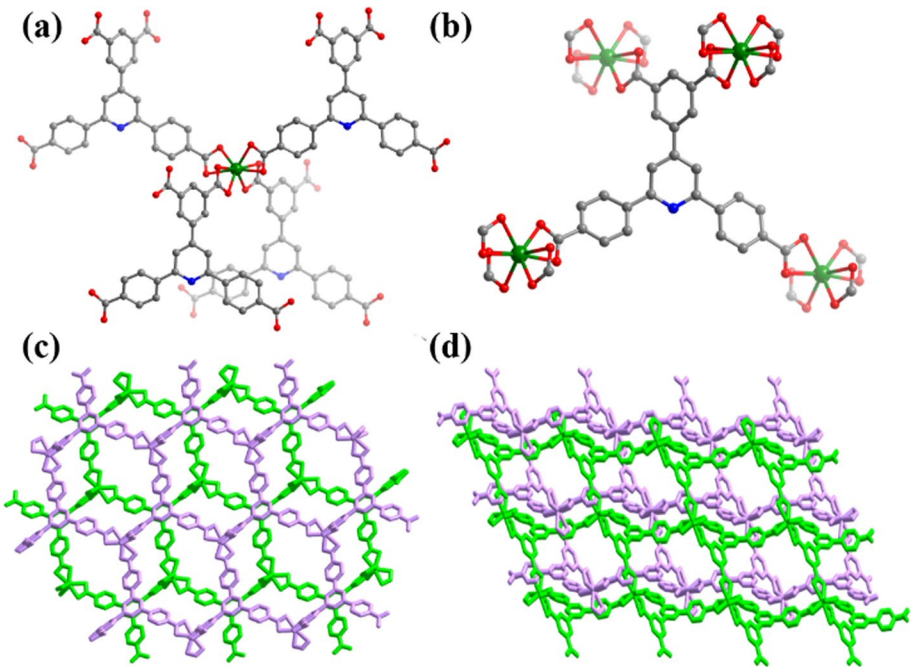

Fig. 2 Coordination modes of **a** $[In(CO_2)_4]$ SBU and **b** $BAPIA^{4-}$ ligand (color code: In, green; C, gray; O, red; and N, blue); a view of the 3D framework of V-101 along the **c** *a* axis and **d** *b* axis, respectively

pretreatment process [19], fluorescence titration experiments were conducted in both water and methanol, respectively. The excitation of V-101 in water and methanol occurred at around 275 nm, and V-101 showed a strong emission peak at 370 nm in water (Fig. S3a). Unexpectedly, V-101 produced an emission peak at 370 nm and a weak emission peak at 475 nm in methanol (Fig. S3b). The weak peak could be assigned to the electron transition of pyridine rings, and similar fluorescence spectra have also been observed for certain pyridyl groups containing polymers [20, 21]. The different emission profiles of V-101 in methanol and in water may be related to the effect of solvent molecules on the structure of V-101 and the polarity of the solvents [22, 23]. With a decrease in solvent polarity, the energy of $\pi \rightarrow \pi^*$ transition increases, and the energy of $n \rightarrow \pi^*$ transition decreases [24]. Therefore, the fluorescence intensity at 370 nm decreased, and the fluorescence intensity at 475 nm increased slightly when the MOF was dispersed in methanol. The SEM images showed that V-101 was uniformly dispersed in solution and formed a good suspension (Fig. S3c and d).

Fluorescence quenching titration experiments were carried out with the incremental addition of aqueous or methanol PFAA solutions to the V-101 suspension in water or methanol. As shown in Fig. 3a–e, with the addition of PFCAs to the water system, the fluorescence emission of V-101 at 370 nm was greatly quenched by short-chain PFCAs (TFA, PFA, PFBA, PFPA, and PFHA), but the fluorescence emission of V-101 at 475 nm increased slightly. In addition, the emission color of V-101 in water changed from blue to turquoise (Fig. 3f). The long-chain PFCAs (PFOA, PFDOA, PFTriDA, and PFTeDA) and two perfluoroalkane sulfonic acids (PFBS and PFOS) showed limited effect on the fluorescence of V-101 (Fig. S4). The quenching efficiencies of short-chain PFCAs (TFA, PFA, PFBA, PFPA, and PFHA) reached 97%, 95%, 91%, 95%, and 73%, respectively, but those of long-chain PFCAs and PFSAs were all lower than 15% (Fig. S5). As shown in Fig. 4a–e, with the addition of PFCAs to the methanol system, the fluorescence emissions of V-101 were significantly enhanced by short-chain PFCAs, and the emission color of V-101 in methanol changed from turquoise to blue (Fig. 4f). Long-chain PFCAs (PFOA, PFDOA, PFTriDA, and PFTeDA) and two PFSAs also had limited effect on the fluorescence of V-101 in the methanol system (Fig. S6). The short-chain PFCAs (TFA, PFA, PFBA, PFPA, and PFHA) enhanced the emissions of V-101 by 14, 8, 19, 9, and 4 times (Fig. S7). Whether in water or in methanol, the fluorescence response of V-101 toward the analytes was almost instantaneous. Furthermore, the fluorescence intensity of V-101 remained basically unchanged with the addition of pure water or pure methanol, which indicated that the fluorescence of V-101 was highly stable (Fig. S8). The above-noted fluorescence changes of V-101 were primarily caused by the addition of short-chain PFCAs.

To better understand the relationship between the concentration of short-chain PFCAs and the fluorescence intensity of V-101, the experimental data obtained in water were fitted with the nonlinear Stern–Volmer (SV) equation.

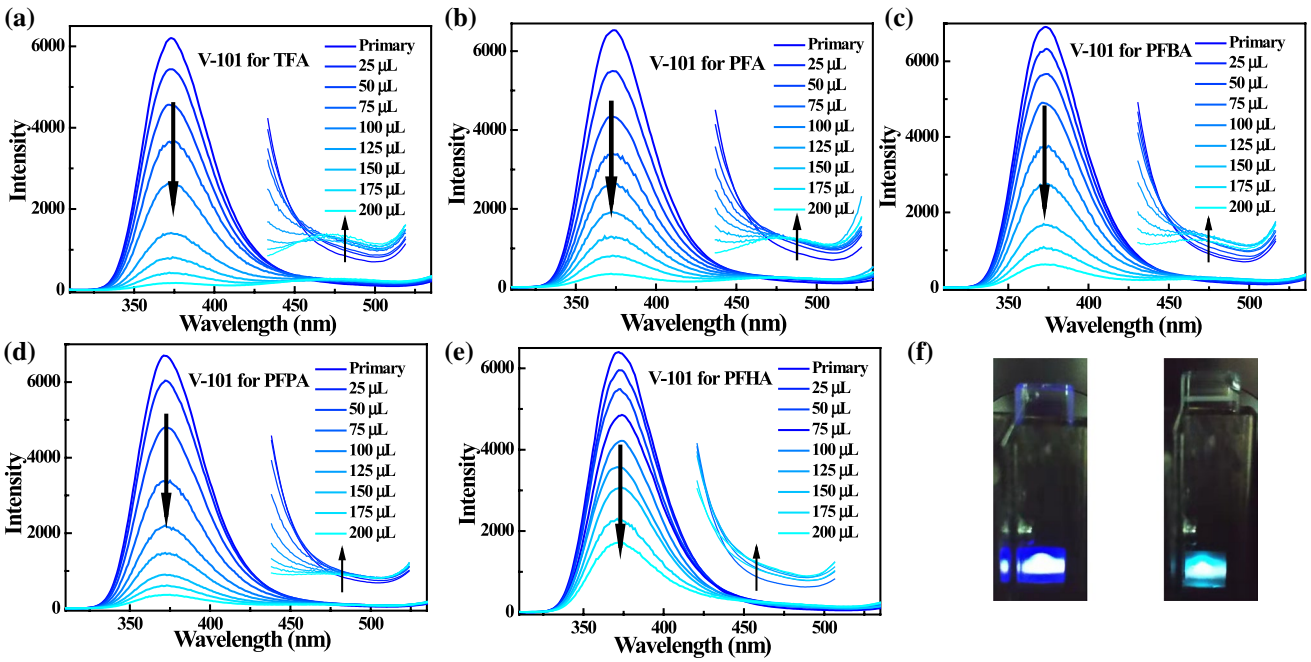

Fig. 3 Effect on emission spectra of V-101 dispersed in water following the incremental addition of 200-μL (100 mg/L) aqueous solution of **a** TFA, **b** PFA, **c** PFBA, **d** PFPA, and **e** PFHA, respectively; **f** left: suspension color of V-101 in water under 275-nm UV light; right: suspension color of V-101 with 200-μL short-chain PFCAs in water under 275-nm UV light

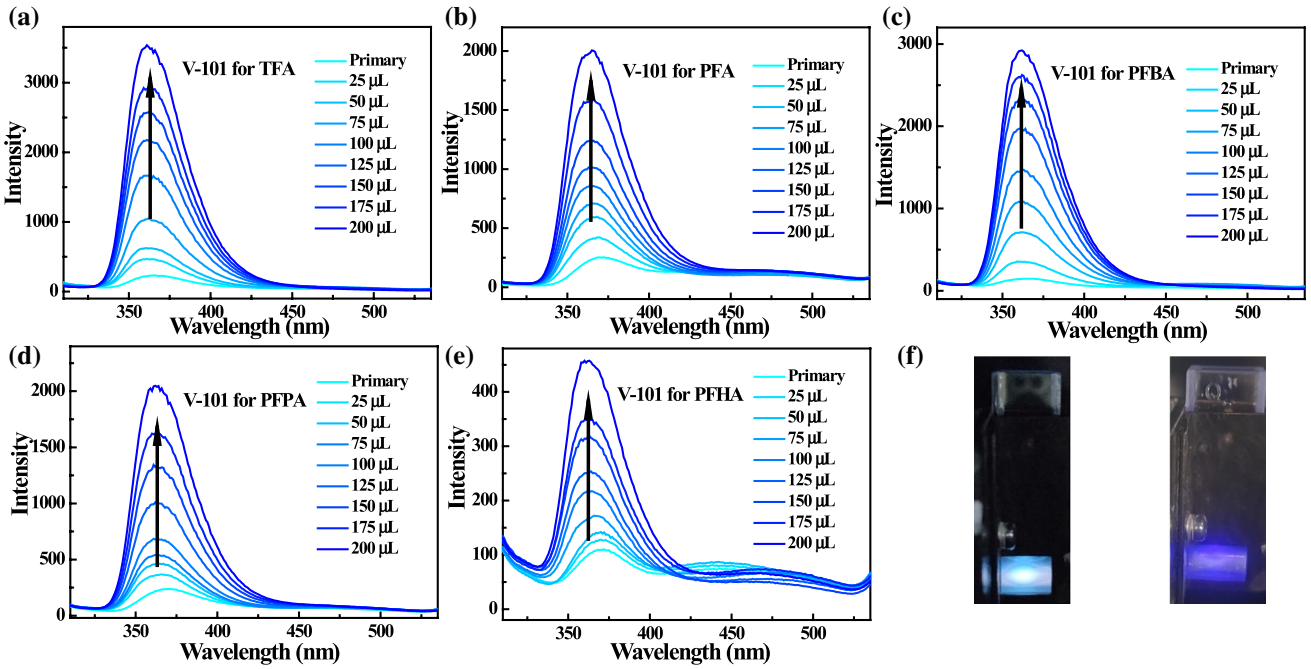

Fig. 4 Effect on emission spectra of V-101 dispersed in methanol following the incremental addition of 200-μL (100 mg/L) methanol solution of **a** TFA, **b** PFA, **c** PFBA, **d** PFPA, and **e** PHA, respectively; **f** left: suspension color of V-101 in methanol under 275-nm UV light; right: suspension color of V-101 with 200-μL short-chain PFCAs in methanol under 275-nm UV light

$$I_0/I = a\exp(k[C]) + b \quad (1)$$

where I_0 is the fluorescence intensity of the initial MOF suspension; I is the fluorescence of the MOF suspension with the addition of PFCAs; K_{sv} is the quenching constant (M^{-1}); $[C]$ is the molar concentration of the specific PFCA; and a, b, and k are constants [25]. The result showed that the relevant data could be perfectly fitted with the nonlinear SV equation, with a correlation coefficient of $R^2 > 0.987$ (Fig. S9). As shown in the insets of Fig. S9, there was a good linear relationship between the concentration of short-chain PFCAs and $I_0/I-1$ of the fluorescence intensity at low concentrations, and it fitted well with the SV equation.

$$I_0/I = K_{sv}[C] + 1 \quad (2)$$

According to $3S_b/K_{sv}$, where S_b is the standard deviation of the blank solutions (Fig. S11), the detection limits of V-101 toward short-chain PFCAs were estimated to be in the range of 8–23 μg/L in water (Table S1). The experimental data tested in methanol were also fitted with the Stern–Volmer equation (Fig. S10). At low concentration ranges, the SV plots for short-chain PFCAs were nearly linear. The detection limits ($3S_b/K_{sv}$) of V-101 toward short-chain PFCAs were estimated to be in the range of 10–146 μg/L in methanol (Table S1).

Anti-interference and selectivity are indispensable properties for sensing probes. To evaluate these properties of V-101, it was dispersed in water and methanol with different metal salts (NaCl, Na_2SO_4, $Mg(NO_3)_2$, $CaCl_2$, NH_4Cl, and KCl), and fluorescence titration experiments were conducted. The experimental results showed that these external ions had a limited impact on the detection performance of V-101 for TFA (Figs. S12a and S13a). The fluorescence spectra of the MOF suspensions were also recorded when the metal salt mixture and the TFA (100 mg/L) were, respectively, added in this order. As shown in Figs. S12b and S13b, with the addition of the mixture, the fluorescence emission of the MOF suspension was unchanged, but the fluorescence intensity of V-101 was significantly quenched or increased when the TFA was added. This indicated that V-101 provided a good anti-interference and selective performance. Furthermore, V-101 samples were collected after the titration experiments to confirm their stability. The PXRD pattern of the tested samples suggested that the samples remained crystalline, and their structure was unchanged after the sensing experiments (Fig. S14).

The Fluorescence Response Mechanism

To unveil the mechanism involved in the fluorescence response of V-101 to short-chain PFCAs, interactions between the MOF and analytes were further explored. PFCAs have no UV absorption; therefore, the inner filter effect and fluorescence resonance energy transfer, which occur due to the adsorption spectrum of analytes overlapping

with the excitation and/or emission spectrum of the fluorescent probes, were first excluded [14, 26]. The prerequisite for the photoinduced electron transfer process is that the energy levels of the lowest unoccupied molecular orbital (LUMO) of the MOF are higher than those of the analytes. The fluorescence of V-101 is mainly derived from the ligand H_4BCPIA; therefore, the HOMO and LUMO energies of H_4BCPIA and PFCAs were calculated using the density functional theory (DFT)-B3LYP/6-31 g* method with Materials Studio software. As shown in Table S2 and Fig. S15, the LUMO orbital energies of PFCAs were higher than those of H_4BCPIA, which suggested that the electrons cannot transfer from excited MOF to PFCAs. As short-chain PFCAs had a similar effect on the fluorescence change of V-101 in both water and methanol, TFA was thus selected as the representative analyte for conducting the further studies presented below to explore the sensing mechanism.

HPLC–MS measurement results revealed that the peak area of fragment ion (CF_3, $m/z = 69$) in the aqueous TFA solution with an original concentration of 10 mg/L was reduced following the addition of V-101, thereby indicating that V-101 adsorbed the TFA molecules in water (Fig. S16). In addition, as discussed above, the experimental data of fluorescence titration in water fitted well with the nonlinear SV equation, and it inferred that the fluorescence quenching of V-101 by TFA was a combined result of both dynamic (collisional) and static quenching; thus, there might be collision and interaction between V-101 and TFA [27].

Compared with the FT-IR spectrum of pristine V-101, FT-IR spectrum of V-101 following immersion in water remained unchanged (Fig. S17). Whereas, obviously there were two new peaks at 1680 and 1230 cm^{-1} in the spectrum of TFA@V-101 (V-101 sample after contact with TFA in water or methanol), which corresponded to the absorption of υ (C=O) bonds of carboxylic acid and σ (N–H) bonds, respectively. This indicated that the TFA molecules were adsorbed by the MOF and that the pyridine N atoms were protonated [16]. According to the results of DFT calculations, the LUMO of H_4BCPIA was obtained from the delocalized π* orbital of the ligand, and the HOMO was obtained from the delocalized π* orbital over the 2, 6-diphenylpyridine moiety, with a certain contribution from a lone orbital pair centered at the pyridine N atom (Fig. 5). After protonation of the pyridine N atom on the ligand, the LUMO of H_5BCPIA$^+$ was unchanged compared with that of H_4BCPIA, and the pyridine N atom did not contribute to the HOMO of H_5BCPIA$^+$. Therefore, the excited state of V-101 shifted from (n, π*) to (π, π*), and the HOMO–LUMO gap changed from 2.967 to 2.602 eV, thereby indicating that the electrons were more likely to transition, and it was also reflected by the appearance of the emission peak at 470 nm and the change in the fluorescence color from blue to turquoise when V-101 was in contact with TFA in water.

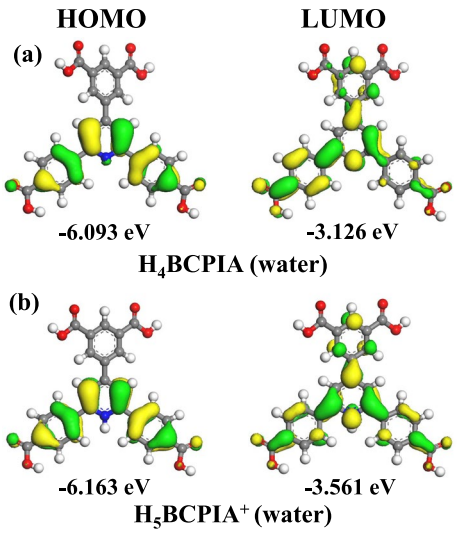

Fig. 5 Frontier molecular orbitals of neutral and protonated forms of H_4BCPIA. **a** H_4BCPIA (water) and **b** H_4BCPIA$^+$ (water)

The N 1 s XPS spectrum of V-101 showed two deconvoluted peaks at 398.3 eV and 401.8 eV, which could be assigned to the aromatic N atoms of pyridine groups and the aliphatic N atoms of $Me_2NH_2^+$ cations, respectively (Fig. S18). A new peak at 399.3 eV corresponding to the protonated pyridine N atoms (N–H) was also observed on the N 1 s XPS spectra of TFA@V-101 (Fig. S19), confirming that a hydrogen bonding interaction occurred between TFA and V-101, and this induced the adsorption behavior. The fluorescence lifetime of the TFA@ V-101 suspension (2.52 ns) was shorter than that of the V-101 suspension (2.97 ns) (Fig. S20). Therefore, the molecular collision between TFA and V-101 and the adsorption of TFA by V-101 may have caused the fluorescence quenching of V-101.

The HPLC–MS analysis results revealed that V-101 also adsorbed TFA in methanol (Fig. S21). Compared to the FT-IR spectra of pristine V-101, a sole new peak at 1680 cm^1 (υ(C=O)) appeared in the spectra of TFA@V-101 obtained in methanol (Fig. S22), and no new peak was observed in the N 1 s XPS spectra (Fig. S23). This indicated that the pyridine N atom in the ligand contributed minimally to the adsorption behavior of V-101 toward TFA in methanol. In addition, the fluorescence lifetime of the TFA@V-101 suspension (2.31 ns) was longer than that of the V-101 suspension (1.52 ns) (Fig. S24). To clearly understand the mechanism involved in fluorescence enhancement, the adsorption behavior of V-101 toward TFA in methanol was simulated using the Dmol3 module in the Material Studio. As shown in Fig. 6, the calculation results suggested that the F and O atoms of TFA adsorbed in the V-101 formed multiple weak hydrogen bonds with the phenyl groups of BCPIA^{4-} ligands, with C–H···O and C–H···F distances ranging from 3.3 to

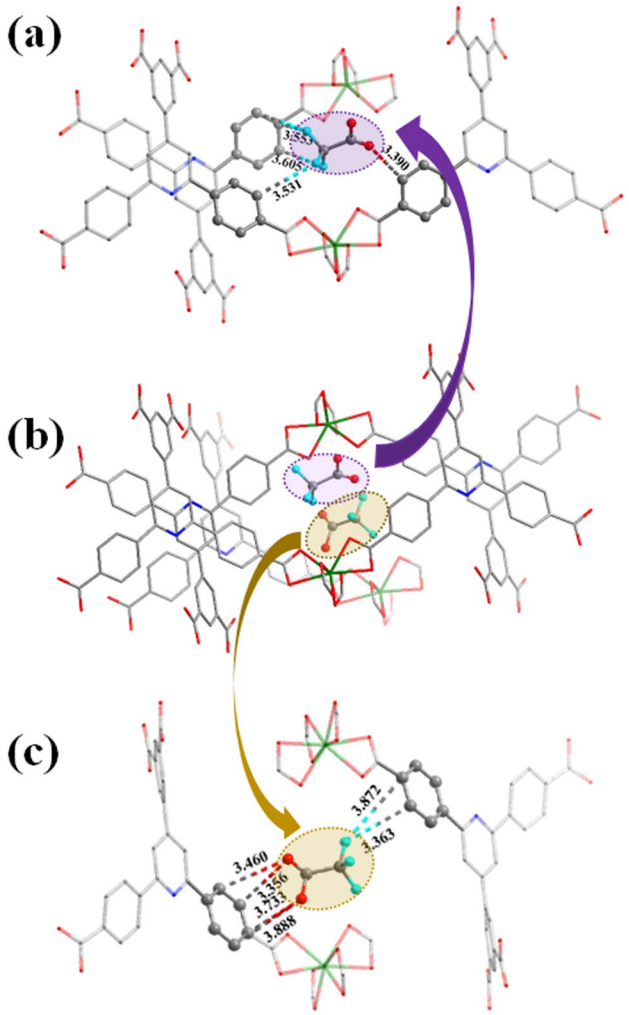

Fig. 6 **a**, **c** Highlighted view of hydrogen bonding between TFA molecules and $BCPIA^{4-}$ ligand, and **b** adsorption sites of TFA molecules after being adsorbed by V-101 in methanol. Color code: In, green; N, blue; O, red; C, gray; and F, wathet blue

3.9 Å [28], which could have restricted rotation of the phenyl rings and thus enhanced the fluorescence of V-101 [29, 30].

As for long-chain PFCAs, the HPLC–MS measurement results revealed that the peak area of fragment ion ($CF_3(CF_2)_6$, $m/z = 370$) of PFOA in water or in methanol became larger after the addition of V-101 (Figs. S25 and S26). This indicated that V-101 could not adsorb PFOA, potentially because the PFOA molecule is too large and the interaction between V-101 and long-chain PFCAs is weak; therefore, the fluorescence of V-10 cannot be quenched by long-chain PFCAs.

In comparison, the ligand H_4BCPIA and two specially reported MOFs (namely, BUT-174, which had the same structure as V-101 but with a different ligand [31], and BUT-16 constructed using Zr^{4+} and $BCPIA^{4-}$ [32]) were selected to detect short-chain PFCAs. As shown in Figs. S27–S29, the ligand and the two reference MOFs were not sensitive to the addition of TFA, and their fluorescence did not change as significantly as that of V-101. It is suggested that the fluorescence response of V-101 to short-chain PFCAs is special, and the MOF is potential useful in the detection of short-chain PFCAs.

According to the literature reports, PFCAs have been detected in water and toilet paper [2, 9, 33]. To evaluate the detection performance of V-101 in real samples, fluorescence titration experiments were conducted 3 times using water from Moon Lake at Beijing University of Technology and methanol extracts from toilet paper. The results showed that V-101 maintained a sensitive fluorescence response to the addition of TFA in both real water and methanol extracts (Fig. S30). This indicates that V-101 has a good application prospect in the detection of short-chain PFCAs. Significantly, the content of PFCAs in the real sample was at the ng/L level; therefore, the detection limits of V-101 require improvement. However, V-101 showed a rapid fluorescence response toward PFCAs, and the system is easy it will be more suitable for the fast and large-scale screening of relatively high concentration of PFCAs in industrial waste.

Conclusions

In summary, it has been demonstrated that an In (III)-based MOF, V-101, has a high potential for use in the fluorescence detection toward short-chain PFCAs in both water and methanol. Due to its fluorescence turn-off, the LODs of V-101 to TFA, PFA, PFBA, PFPA, and PFHA ranged from 8 to 23 μg/L in water and from 10 to 146 μg/L in methanol due to its fluorescence turn-on. Moreover, V-101 also exhibited excellent anti-interference abilities toward PFCAs in the presence of many common metal ions. The pyridine N atom in V-101 was found to play an important role in changing the fluorescence color of the material following analyte addition, and the collision and interaction between the MOF and the analyte were found to be the major mechanisms involved in changes in the fluorescence intensity of V-101. This work provides important information about the detection ability of LMOFs toward short-chain PFCAs. LMOFs provide a pre-enrichment effect, and their response is sensitive and involves a visible color change. The associated equipment required is simple to operate, making them potential candidates for the sensing of hazardous pollutants even those without aromatic rings.

Supplementary Information The online version contains supplementary material available at https://doi.org/10.1007/s12209-023-00356-z.

Acknowledgements We would like to acknowledge the financial support from the National Natural Science Foundation of China (Nos. 22225803 and 22038001).

Author Contributions JL helped in conceptualization, methodology, investigation, and writing—original draft. YX worked in visualization, supervision, and formal analysis. LX helped in writing—review and editing and supervision. JL worked in supervision and funding acquisition.

Declarations

Conflicts of interest The authors declare no competing financial interests or personal relationships that could have appeared to influence the work reported in this work.

References

1. Prevedouros K, Cousins IT, Buck RC et al (2006) Sources, fate and transport of perfluorocarboxylates. Environ Sci Technol 40(1):32–44
2. Krafft MP (2015) Selected physicochemical aspects of poly- and perfluoroalkylated substances relevant to performance, environment and sustainability-part one. Chemosphere 129:4–19
3. Stanifer JW, Stapleton HM, Souma T et al (2018) Perfluorinated chemicals as emerging environmental threats to kidney health: a scoping review. Clin J Am Soc Nephrol 13(10):1479–1492
4. Gebbink WA, Berger U, Cousins IT (2015) Estimating human exposure to PFOS isomers and PFCA homologues: the relative importance of direct and indirect (precursor) exposure. Environ Int 74:160–169
5. Chow SJ, Croll HC, Ojeda N et al (2022) Comparative investigation of PFAS adsorption onto activated carbon and anion exchange resins during long-term operation of a pilot treatment plant. Water Res 226:119198
6. Venkatesan AK, Halden RU (2014) Loss and in situ production of perfluoroalkyl chemicals in outdoor biosolids-soil mesocosms. Environ Res 132:321–327
7. Lena V (2014) Transport of perfluoroalkyl acids in a water-saturated sediment column investigated under near-natural conditions. Environ Pollut 186:7–13
8. Barisci S, Suri R (2020) Electrooxidation of short and long chain perfluorocarboxylic acids using boron doped diamond electrodes. Chemosphere 243:125349
9. Zhanyun W (2015) Hazard assessment of fluorinated alternatives to long-chain perfluoroalkyl acids (PFAAs) and their precursors: status quo, ongoing challenges and possible solutions. Environ Int 75:172–179
10. Zhang QH, Wang P, Li XM et al (2019) Analysis of perfluoroalkyl and polyfluoroalkyl compounds. Methods of analysis and detection of persistent organic pollutants. Academic Press, Beijing, pp 169–194
11. Hitabatuma A, Wang PL, Su XO et al (2022) Metal-organic frameworks-based sensors for food safety. Foods 11(3):382
12. Weiwei C (2021) Applications of metal-organic framework (MOF)-based sensors for food safety: enhancing mechanisms and recent advances. Trends Food Sci Technol 112:268–282
13. Hu ZC, Deibert BJ, Li J (2014) Luminescent metal-organic frameworks for chemical sensing and explosive detection. Chem Soc Rev 43(16):5815–5840
14. Lustig WP, Mukherjee S, Rudd ND et al (2017) Metal-organic frameworks: functional luminescent and photonic materials for sensing applications. Chem Soc Rev 46(11):3242–3285
15. Li R, Alomari S, Stanton R et al (2021) Efficient removal of per- and polyfluoroalkyl substances from water with zirconium-based metal-organic frameworks. Chem Mater 33(9):3276–3285
16. Yin HQ, Tan K, Jensen S et al (2021) A switchable sensor and scavenger: detection and removal of fluorinated chemical species by a luminescent metal-organic framework. Chem Sci 12(42):14189–14197
17. Hou SL, Dong J, Jiang XL et al (2018) Interpenetration-dependent luminescent probe in indium-organic frameworks for selectively detecting nitrofurazone in water. Anal Chem 90(3):1516–1519
18. Wang B, Yang H, Xie Y-B et al (2016) Controlling structural topology of metal-organic frameworks with a desymmetric 4-connected ligand through the design of metal-containing nodes. Chin Chem Lett 27(4):502–506
19. Lorenzo M, Campo J, Picó Y (2015) Optimization and comparison of several extraction methods for determining perfluoroalkyl substances in abiotic environmental solid matrices using liquid chromatography-mass spectrometry. Anal Bioanal Chem 407(19):5767–5781
20. Zhang Y, Murphy CB, Jones WE (2002) Poly[*p*-(phenyleneethynylene)-*alt*-(thienyleneethynylene)] polymers with oligopyridine pendant groups: highly sensitive chemosensors for transition metal ions. Macromolecules 35(3):630–636
21. Wang B, Yang Q, Guo C et al (2017) Stable Zr(IV)-based metal-organic frameworks with predesigned functionalized ligands for highly selective detection of Fe(III) ions in water. ACS Appl Mater Interfaces 9(11):10286–10295
22. Khatua S, Biswas P (2020) Flexible luminescent MOF: trapping of less stable conformation of rotational isomers, in situ guest-responsive turn-off and turn-on luminescence and mechanistic study. ACS Appl Mater Interfaces 12(19):22335–22346
23. Khatua S, Goswami S, Biswas S et al (2015) Stable multiresponsive luminescent MOF for colorimetric detection of small molecules in selective and reversible manner. Chem Mater 27(15):5349–5360
24. Xu JG, Wang ZB (2006) Effects of environmental factors on fluorescence spectra and fluorescence intensity. Fluorescence analysis method. Academic Press, Beijing, pp 49–62
25. Wang L, Fan GL, Xu XF et al (2017) Detection of polychlorinated benzenes (persistent organic pollutants) by a luminescent sensor based on a lanthanide metal-organic framework. J Mater Chem A 5(11):5541–5549
26. Baheti A, Vigalok A (2019) Short wavelength inner filter technique (SWIFT) in designing reactive fluorescent molecular probes. J Am Chem Soc 141(31):12224–12228
27. Zhao DH, Swager TM (2005) Sensory responses in solution vs solid state: a fluorescence quenching study of poly (iptyceneb-utadiynylene) S. Macromolecules 38(22):9377–9384
28. Su CY, Pan M (2010) Weak interactions in supramolecular systems–intermolecular bonds. The basis and progress of coordination supramolecular structural chemistry. Science Press, Beijing, pp 43–86

29. Che G, Gu DX, Yang WT et al (2022) Turn-on fluorescence detection of acetic acid in wine using a uranyl-organic framework. Cryst Growth Des 22(3):1984–1990
30. Qiao JY, Liu XY, Zhang LR et al (2022) Unique fluorescence turn-on and turn-off-on responses to acids by a carbazole-based metal-organic framework and theoretical studies. J Am Chem Soc 144(37):17054–17063
31. Lv J, Wang B, Li JY et al (2022) Detection of toxic polychlorinated biphenyls by nanoporous metal-organic frameworks. ACS Appl Nano Mater 5(8):11656–11664
32. Cheng J, Wang B, Lv J et al (2021) Remarkable uptake of deoxynivalenol in stable metal-organic frameworks. ACS Appl Mater Interfaces 13(48):58019–58026
33. Thompson JT, Chen BT, Bowden JA et al (2023) Per- and polyfluoroalkyl substances in toilet paper and the impact on wastewater systems. Environ Sci Technol Lett 10(3):234–239

Lin-Hua Xie obtained his Ph.D. in 2010 from Sun Yat-Sen University under the supervision of Prof. X.-M. Chen. After postdoctoral research at Seoul National University in Prof. M. P. Suh's group from 2010 to 2012 and at King Abdullah University of Science and Technology in Prof. Z. Lai's group from 2012 to 2015, he joined Beijing University of Technology as an associate professor. His research interests include the functionalization and application of new porous materials.

Jian-Rong Li obtained his Ph.D. in 2005 from Nankai University under the supervision of Prof. X.-H. Bu. Until 2008, he was an assistant professor at the same university. From 2008 to 2012, he has been a postdoctoral research associate and then assistant research scientist at Texas A&M University in Prof. H.-C. Zhou's group. Since 2011, he has been a full professor at Beijing University of Technology. His research interest focuses on porous materials for chemical engineering, energy, and environmental science. He has published ten book chapters and over 330 papers (> 36,000 citations) and has been selected as a Web of Science Highly Cited Researcher from 2017 to 2022.